Journal of Thermal Analysis, Vol. 52 (1998) 729-737

MICRO-EFFECTS ON CONTINUOUS-INJECTION HEAT CONDUCTION CALORIMETRY

F. Socorro and M. Rodríguez de Rivera

ETSII, Universidad de Las Palmas, Campus de Tafira, E-35017 Las Palmas de Gran Canaria Spain

Abstract

A localized-constant model involving two capacities reliably describes two injection calorimeters: a mass-variation calorimeter and a constant-volume calorimeter (TAM 2277 by Thermometric). The model distinguishes the place and the types of dissipation, and its parameters depend on the rates and on the heat capacities of the liquids. In the case of the TAM 2277 calorimeter, the dependence between the detected heat of mixing and the injection rate is revealed. The proposed model permits the inclusion of perturbations on the baseline originating from the temperature variation of the thermostat.

Keywords: conduction calorimetry, flow calorimetry, liquid mixtures, low concentration, modelling, signal processing, time-dependent systems

Introduction

Continuous-injection heat conduction calorimeters are used for the thermodynamic study of liquid mixtures. Identification of the calorimetric model and appropriate signal processing of the experimental measurements permit the determination of thermodynamic properties of mixtures and solutions. Starting from a localized-constant model, we try to explain some perturbations in two injection calorimeters: a mass-variation calorimeter [1] and a constant-volume calorimeter [2] (TAM 2277 by Thermometric). The former provides good results for the overall mole fraction domain ($0.001 \leq x_i \leq 0.999$), the low concentration zone being especially interesting; the latter is suitable for intermediate concentrations ($0.15 \leq x_i \leq 0.85$).

The principle of performance of injection and mass-variation calorimeters consists in the continuous injection of a liquid into another one situated in the laboratory cell. The heat of mixing is in relation to the dissipation $W(t)$, supposing that, at each instant, equilibrium is reached and the mixture is perfectly homogeneous. The thermodynamic property under consideration is obtained as a continuous function of the concentration [3] and its accuracy will depend on the precision of n_1, n_2 and the model chosen to determine $W(t)$ from the experimental

1418–2874/98/ $ 5.00

Akadémiai Kiadó, Budapest
Kluwer Academic Publishers, Dordrecht

curve. Models with three and six heat capacities with variable parameters have been proposed [4–6], the injection effect has been demonstrated [7, 8] and there are even works that consider the variation in the sensitivity with the level of liquid in the cell [8]; recently, due to improvements in temperature control, non-differential calorimeters have been proposed [9]. Here we will prove that a two-capacity model is sufficient to describe the typical phenomena of the variability of the system and the micro-effects detected in the calibration:

a) The injection causes an increase in the heat capacity of the contents of the laboratory cell, and as a consequence an increase in the main time constant. The thermal coupling and the detection surface grow larger with the volume, causing a variation in the sensitivity.

b) An additional energetic term appears, due to the temperature difference between the injected liquid and the mixture.

c) If volatile liquids are used, then the vaporization heat included in the power $W(t)$ will produce a certain imprecision in the determination of n_1 and n_2.

d) In this calorimeter, the calibration resistance is situated in the liquid, and the difference between the electric and the chemical calibrations is not appreciated (it is presumed that the dissipated power does not perceptibly modify the temperature of the thermostat)

In the injection and constant-volume calorimeter (TAM 2277 by Thermometric), the reaction zone has three orifices: two for injecting the liquid in continuous form, and one as exit. The heat of mixing is calculated when the experimental output reaches the permanent state. Now we do not obtain a continuous function, but distinct values for each molar fraction x_i that match up to the programmed rates of each injector. The detection surface of these instruments is constant and no vapour space is present. Nowadays, this device provides reliable thermodynamic results of excess enthalpies of liquid mixtures [10, 11]; the calibrations are based on determination of the sensitivity as function of the injection rates and the heat capacities of the liquids used [12–14]; instruments are now being constructed in which the reaction zones are of higher volume and in which the influence of the rate is less [15]. This calorimeter (TAM 2277) has also been used for the determination of heat capacities C_p; in this case, a second-order model was chosen [16]. Here, we consider that a two-capacity model adequately describes the performance of the device; three micro-effects are taken into account:

a) energetic terms due to friction and to the temperature difference between the injected liquid and the mixture;

b) the difference between the chemical and the electric calibration (this is because the Joule dissipation is not produced in the same place as the mixing),

c) the mixing could continue out of the detection zone, due to the increasing injection rate.

In this work, an experimental analysis of the described micro-effects is performed, and an acceptable explanation is given via a very simple modellization of these instruments.

Model and experimental measures

Injection and mass-variation calorimeter

For a correct reconstruction of the power $W(t)$ from the curves $y(t)$, a model is needed that faithfully represents the experimental device. A model of six heat capacities is adequate [6], although it is possible to design simpler equivalent models with three heat capacities [17]. The signal-noise relation will determine the size of the model. In order to explain the typical variability phenomena of the system, a model of two heat capacities has been chosen. Figure 2A represents the experimental transfer function (TF), and the TF of two simple models (one with three bodies and another with two bodies).

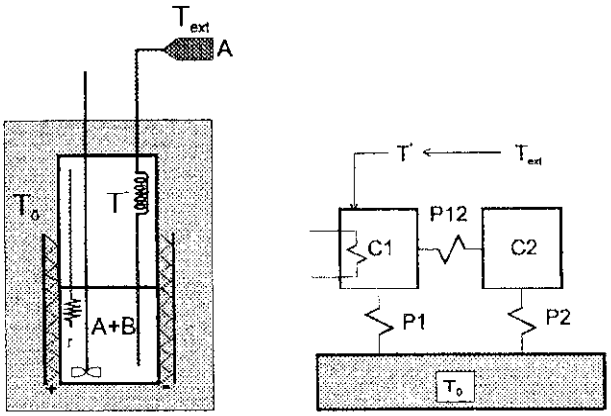

Fig. 1 Scheme and model for an injection and mass-variation calorimeter. T_0 is the thermostat temperature, T_{ext} is the outside temperature and T^* is the temperature reached by the liquid before entering the cell. r is the resistance for the electric calibration

Figure 1 shows a scheme of the device and of the associated model where the dissipation takes place in the first body: $W=W_{mix}+W_{joule}+W_{vaporization}$, and the calorimetric output is proportional to the temperature difference (T_1-T_0), and to the detection surface A: $y_1(t)=KA(T_1-T_0)$. The equations of the model are as follows:

$$W(t) = C_1\frac{dT_1}{dt} + P_{12}(T_1-T_2) + P_1(T_1-T_0) + \frac{dC}{dt}(T_1-T^*)$$

$$0 = C_2\frac{dT_2}{dt} + P_{12}(T_2-T_1) + P_2(T_2-T_0)$$

where C_1 and C_2 are the heat capacities of the 1st and 2nd elements, P_1 and P_2 are the inverses of the thermal resistances between the 1st and 2nd elements and the thermostat, and P_{12} is the inverse of the thermal resistance between the 1st and 2nd elements. T_1 and T_2 are the temperatures of the 1st and 2nd elements.

The temperature of the injected liquid, T^*, depends on the injection rate v:

$$T_0-T^* = (T_0-T_{ext})(1-e^{-\gamma v}) = \Delta T_{CTR}(1-e^{-\gamma v}).$$

The variable parameters undergo linear change [20]:

$$C_1 = C_{10} + \alpha_C V \qquad \text{for } V_0<V<V_M$$
$$P_1 = P_{10} + \alpha_P V \qquad \text{for } V_0<V<V_M$$
$$A = A_0 + \alpha_A V \qquad \text{for } V_0<V<V_T \text{ (thermopile zone)}$$
$$A = A_0 + \alpha_A V_T \qquad \text{for } V_T<V<V_M$$

α_C, α_P and α_A depend on the injection rate; V is the volume, and V_0 and V_M are the minimum and maximum volumes in the cell.

The power $W(t)$ and the thermogram $y_1(t)$ are connected as follows:

$$a_1\frac{dW^*(t)}{dt} + a_0W^*(t) = b_2(t)\frac{d^2y_1(t)}{dt^2} + b_1(t)\frac{dy_1(t)}{dt} + b_0(t)y_1(t)$$

$$W^*(t) = W(t)-C\Delta T_{CTR}(1-e^{-\gamma v})$$

Experimental results

1) Our model of two heat capacities has a TF with two poles in the invariant situation. Although it does not exactly represent the experimental TF, it is sufficient to obtain an acceptable approximation to the heat of mixing as a function of time [17]. Figure 2B shows the variation of τ_1 with the volume.

2) The variation in sensitivity with the liquid level (Fig. 2C) is justified by the variability of A and P_1:

$$S = \frac{KA(P_{12}+P_2)}{(P_{12}+P_2)P_1 + P_2P_{12}}$$

(observe that, if there is only one body, $P_2=0$ and then $S=KA/P_1$).

3) The model considers the injection effect; to evaluate it, the same liquid is injected when the response to electric dissipation reaches the permanent state. At a rate of 3 $cm^3\ h^{-1}$ for cyclohexane, the diminution of the calorimetric output is 0.7%, at 9 $cm^3\ h^{-1}$ it is 2.3% and at 15 $cm^3\ h^{-1}$ it is 4.6%. This demonstrates that, when the rate is increased, the contribution of the term $C\Delta T_{CRT}(1-e^{-\gamma v})$ is more important (Fig. 3).

$$y_1 = KA\frac{[W-\dot{C}\Delta T_{CRT}(1-e^{-\gamma v})](P_{12}+P_2)}{(P_{12}+P_2)(P_1+\dot{C})+P_2P_{12}}$$

(if P_2=0, then y_1=$KAW^*/(P_1+\dot{C})$.

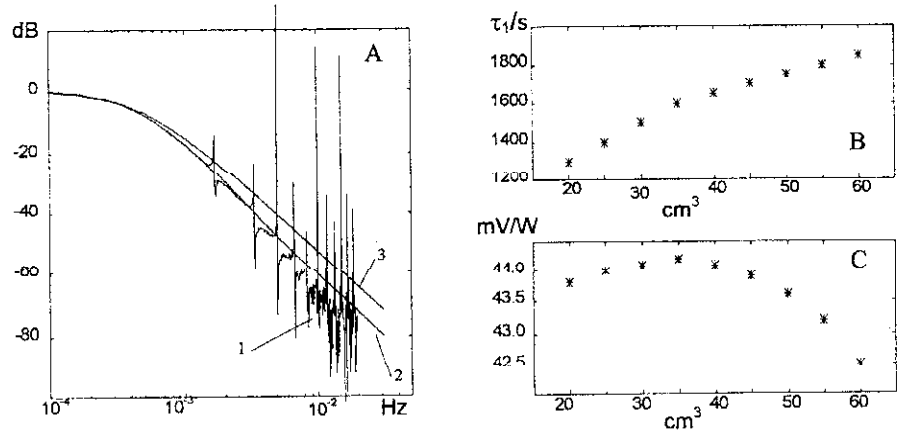

Fig. 2 Injection and mass-variation calorimeter. A) Curve 1 is the frequential representation of the experimental transfer function, obtained from the response to an electric pulse of 10 min duration (for 20 cm^3 of benzene) [19]. Curve 2 matches up to a three-pole and a zero TF (τ_1=540, τ_2=210, τ_3=140, τ_1^*=55) and curve 3 to a two-pole TF (τ_1=540, τ_2=210); these values were obtained by inverse filtering [21]. Experimental values of the first time constant (B) and of the sensitivity (C), both as functions of the volume (cell contents: water)

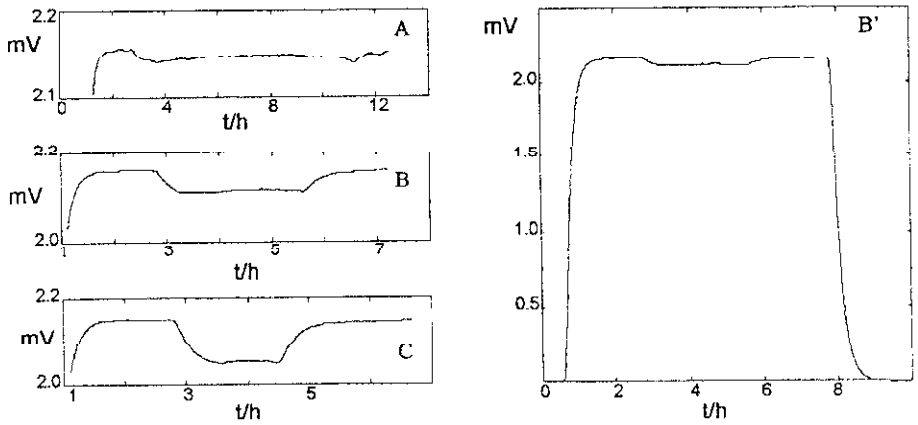

Fig. 3 Injection and mass-variation calorimeter. Experimental evaluation of the injection effect. B') Signal corresponding to electric dissipation during which 24 cm^3 of cyclohexane was injected into 20 cm^3 of cyclohexane (9 $cm^3\,h^{-1}$). Enlargement of the injection area for the rates: 3 $cm^3\,h^{-1}$ (A), 9 $cm^3\,h^{-1}$ (B) and 15 $cm^3\,h^{-1}$ (C)

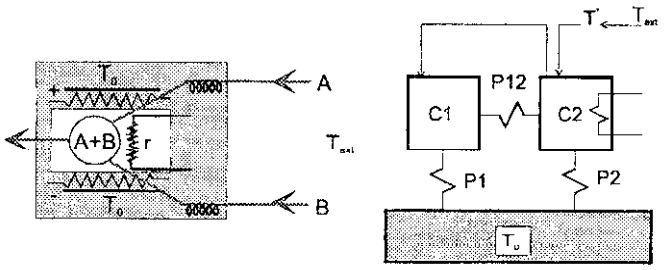

Fig. 4 Scheme and model corresponding to the TAM 2277 calorimeter. T_0 is the thermostat temperature, r is the calibration resistance, T_{ext} is the outside temperature and T^* is the temperature at which the injected liquid reaches domain 2

Further, the output for a 'pseudo-permanent' injection follows the variation in sensitivity for volumes between 20 and 44 cm^3; the same form is observed in the curves reported by Rey *et al.* [7].

Injection and constant-volume calorimeter (TAM 2277)

In this case, the Joule dissipation does not occur at the same place as the mixing. Additionally, experimental measurements show that the injected liquid passes near the calibration resistance before reaching the reaction zone (Fig. 4 and curve b5 of Fig. 5B).

$$W_1(t) = C_1\frac{dT_1}{dt} + P_{12}(T_1-T_2) + P_1(T_1-T_0) + \frac{dC}{dt}(T_1-T_2)$$

$$W_2(t) = C_2\frac{dT_2}{dt} + P_{12}(T_2-T_1) + P_2(T_2-T_0) + \frac{dC}{dt}(T_2-T^*)$$

where $W_1(t)=W_{friction}+W_{mix}\,e^{-\beta(vA+vB)}$ and $W_2(t)=W_{Joule}$.

The calorimetric output and temperature difference between the thermostat and the injected liquid are given by the expressions

$$y_1(t) = KA(T_1-T_0)$$

$$T_0-T^* = (T_0-T_{ext})(1-e^{-\gamma v}) - \Delta T_{CTR}(1-e^{-\gamma v})$$

Only the curve in the permanent state is of interest ($dT_1/dt=dT_2/dt=0$:

$$y_1 = KA\frac{W_1(P_{12}+P_2+\dot{C}) + [W_2-\dot{C}\Delta T_{CRT}(1-e^{-\gamma v})](P_{12}+\dot{C})}{(P_{12}+P_1+C)(P_2+C)+P_1P_{12}}$$

Experimental results

a) Injection effect. Figure 5 shows the curve corresponding to injections of cyclohexane + cyclohexane during constant electric dissipation. For different in-

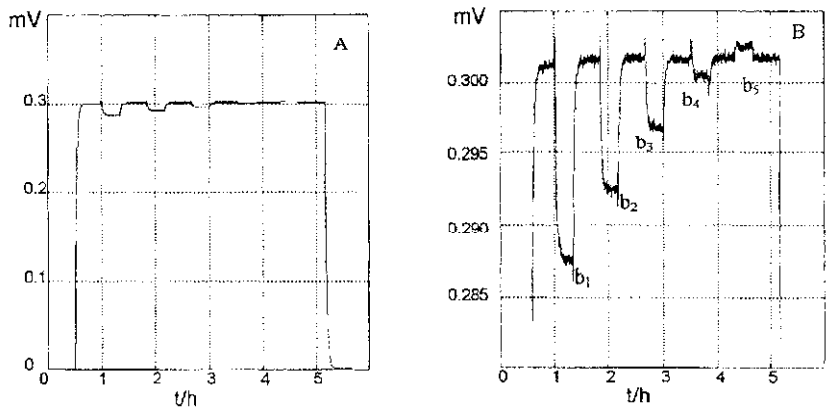

Fig. 5 TAM 2277 calorimeter. A) Experimental curve corresponding to injections of cyclohexane into cyclohexane during electric dissipation, for different injection rates v_A+v_B=60 (b1), 48 (b2), 36 (b3), 24 (b4) and 12 cm^3 h^{-1} (b5) ($v_A=v_B$). B) Enlargement of injection zones

jection rates v_A+v_B=60, 48, 36, 24 and 12 cm^3 h^{-1}, the calorimetric output is modified by −4.8, −3.1,−1.6, 0.4 and 10.3%. This result is coherent with the model: for the smallest rate, the effect of $C\Delta T_{CRT}(1-e^{-\gamma v})$ is insignificant and the output y_1 (with injection) is then greater than y_1^0 (without injection). In this comparative study, $W_{friction}$ has been considered exiguous.

$$y_1 = KA\frac{W_2(P_{12}+C)}{(P_{12}+P_1+C)(P_2+C)+P_1P_{12}} \text{ (with injection)}$$

$$y_1^0 = KA\frac{W_2P_{12}}{(P_{12}+P_1)(P_2+P_1P_{12}} \text{ (without injection)}$$

b) Figure 6 shows the friction effect; on injection of cyclohexane + cyclohexane at the rates v_A+v_B=60, 48, 36, 24 and 12 cm^3 h^{-1}, the dissipated powers are 4.9, 3.8, 2.2, 1.6 and 0.3 μW ($v_A=v_B$).

c) There is a slight difference between the sensitivity obtained with the electric calibration (S_e) and that obtained with the chemical calibration (S_q) because the dissipation by the Joule effect does not take place in the same zone as that where the mixture is produced. The model foresees this and, considering the term $C\Delta T_{CRT}(1-e^{-\gamma v})$ to be insignificant, we have $S_e<S_q$:

$$S_e = \frac{y_1}{W_2} = KA\frac{P_{12}}{(P_{12}+P_1)P_2+P_1P_{12}} \text{ (without injection)}$$

$$S_q = \frac{y_1}{W_1} = KA\frac{(P_{12}+P_2+C)}{(P_{12}+P_1+C)(P_2+C)+P_1P_{12}}$$

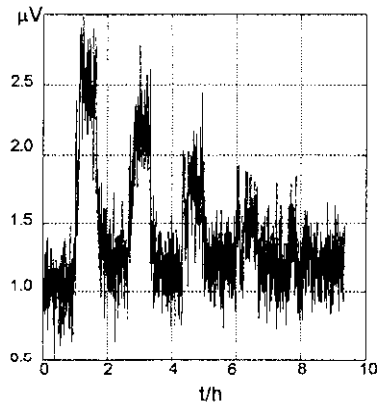

Fig. 6 TAM 2277 calorimeter. Response to the injection of cyclohexane + cyclohexane for v_A+v_B=60, 48, 36, 24 and 12 $cm^3\ h^{-1}$ ($v_A=v_B$)

The following experimental values are deduced from the calibrations: S_c=313.0 mV W^{-1} and S_q=313.6 mV W^{-1} (for hexane(1) + cyclohexane(2) with v_1+v_2=12 $cm^3\ h^{-1}$).

Table 1 Detected power on increase of the injection rate ($v_1=v_2$)

Hexane (1) + cyclohexane (2) $H^E(x_1)$ ref.=220.3 J mol^{-1} [18] x_1=0.4525			
v_1+v_2 (cc/h)	n_1+n_2 (μmol/s)	mW exp.	error in % (*)
11.96	0.0282	6.2117	–0.01
23.94	0.0564	12.3629	–0.50
35.90	0.0846	18.3450	–1.57
47.86	0.1128	24.0976	–3.03
59.84	0.1409	29.6110	–4.60

(*) in relation to the theoretical power that should be detected to obtain H^E ref.

d) Finally, it is very important to emphasize that, when the injection rate is increased, the detected heat of mixing diminishes, increasing the error (Table 1). This is principally due to the injection effect.

Conclusions

Modellization of these instruments is essential for a correct identification of the system and, as a consequence, for a reliable calculation of the heat of mixing to be determined. The analysis reveals that the injection effect must be included in the calibration of the calorimeter. It is also concluded that the maximum injection rates are determined by two aspects:

a) The term $\dot{C}\Delta T_{CRT}(1-e^{-\gamma v})$ must be minimized in both calorimeters. An adequate cooling coil is therefore used to homogenize the temperatures of the liquids before they reach the reaction zone.

b) In the TAM 2277 calorimeter, it must be ensured that the mixture is produced in the reaction zone, which limits the injection rates. A volume increase in the reaction zone elevates the probability of the mixing taking place in the mentioned domain, so that the rates can increase.

In the mass-variation calorimeter, the rate limit is imposed by aspect a). In our device, it is recommended to inject at rates less than 9 $cm^3\ h^{-1}$. In the TAM 2277 calorimeter, the rate limit is imposed by the second aspect; in our case, rates $v_i<18\ cm^3\ h^{-1}$ are recommended. In both cases, however, even at these rates, the injection effect must be corrected.

References

1 F. Socorro, M. Rodríguez de Rivera, J. P. Dubés, H. Tachoire and V. Torra, Meas. Sci. Technol., 1 (1990) 1285.
2 Instruction Manual for 2277 Thermal Activity Monitor (1992), Thermometric AB Sweden.
3 H. Tachoire, J. L. Macqueron and V. Torra, Thermochim. Acta, 105 (1986) 333.
4 E. Cesari, J. Viñals and V. Torra, Thermochim. Acta, 63 (1983) 341.
5 J. Ortin, A. Ramos, V. Torra and J. Viñals, Thermochim. Acta, 75 (1984) 173.
6 M. Rodríguez de Rivera, F. Socorro, J.P. Dubés, H. Tachoire and V. Torra, Thermochim. Acta, 150 (1989) 11.
7 C. Rey, J. R. Rodríguez, V. Pérez-Villar, J. Ortín, V. Torra, J. P. Dubès, R. Kechavarz and H. Tachoire, Thermochim. Acta, 81 (1984) 97.
8 M. Rodríguez de Rivera, H. Tachoire and V. Torra, J. Thermal Anal., 41 (1994) 1385.
9 V. Torra and H. Tachoire, Thermochim. Acta, 266 (1995) 239.
10 Z. Ting, G. C. Benson and B. C.-Y. Lu, Thermochim. Acta, 288 (1996) 29.
11 K. C. Singh, K. C. Kalra, S. Makenand and V. Gupta, Thermochim. Acta, 275 (1996) 51.
12 R. Tanaka, P. J. D'Arcy and G. Benson, Thermochim. Acta, 11 (1975) 163.
13 B. S. Harsted and E. S. Thomsen, J. Chem. Thermodyn., 6 (1974) 549.
14 P. Monk and I. Wadsö, Acta Chem. Scand., 22 (1968) 1842.
15 C. J. Wormald, L. Badock and M. J. Cloyd, J. Chem. Thermodynamics, 28 (1996) 603.
16 B. Löwen, U. Peukert and S. Schulz, Thermochim. Acta, 255 (1995) 1.
17 L. Alvarez, Doctoral thesis, Universidad de Las Palmas (1996).
18 Marsh and Stokes, J. Chem. Thermodyn., 1 (1969) 223.
19 F. Marco, M. Rodríguez de Rivera, J. Ortín and V. Torra, Thermochim. Acta, 89 (1985) 315.
20 F. Marco, M. Rodríguez de Rivera, J. Ortín, T. Serra and V. Torra, Thermochim. Acta, 107 (1986) 149.
21 F. Marco, M. Rodríguez de Rivera, J. Ortín, T. Serra and V. Torra, Thermochim. Acta, 102 (1986) 173.